Deterministic Time-Bin Entanglement between a Single Photon and an Atomic Ensemble

Peng-Fei Sun,[1,2,*] Yong Yu,[1,2,*] Zi-Ye An,[1,2] Jun Li,[1,2] Chao-Wei Yang,[1,2] Xiao-Hui Bao,[1,2] and Jian-Wei Pan[1,2]
[1]Hefei National Laboratory for Physical Sciences at Microscale and Department of Modern Physics, University of Science and Technology of China, Hefei, Anhui 230026, China
[2]CAS Center for Excellence in Quantum Information and Quantum Physics, University of Science and Technology of China, Hefei, Anhui 230026, China

(Received 5 August 2021; accepted 20 January 2022; published 10 February 2022)

Hybrid matter-photon entanglement is the building block for quantum networks. It is very favorable if the entanglement can be prepared with a high probability. In this Letter, we report the deterministic creation of entanglement between an atomic ensemble and a single photon by harnessing the Rydberg blockade. We design a scheme that creates entanglement between a single photon's temporal modes and the Rydberg levels that host a collective excitation, using a process of cyclical retrieving and patching. The hybrid entanglement is tested via retrieving the atomic excitation as a second photon and performing correlation measurements, which suggest an entanglement fidelity of 87.8%. Our source of matter-photon entanglement will enable the entangling of remote quantum memories with much higher efficiency.

DOI: 10.1103/PhysRevLett.128.060502

The construction of quantum networks [1–3] over long distance requires matter qubits with an efficient optical interface, since photons are an excellent candidate for long-distance transmission, and matter qubits are necessary to connect different segments. A paradigm for this situation is an entanglement pair between a single photon and a matter qubit. For application in quantum networks, it is necessary that the hybrid entanglement has a very high preparation efficiency and fidelity, at the same time the matter qubit can be preserved for a long duration [4].

It is very promising of harnessing atomic ensembles [4–6] for quantum networks, since an ensemble of atoms is relatively easier to prepare in comparison with single atoms, and it has the additional advantage of collective enhancement, which enables efficient interaction with single photons. In the past, plenty of effort has been made in improving the performance of laser-cooled atomic ensembles [7–29]. Notably, very high retrieval efficiency has been achieved either by using large optical depth [16,22,24,27] or with the assistance of a low-finesse cavity [7,13,17,29]; subsecond storage has been achieved by confining the atoms with an optical lattice and compensating the differential light shift [11,12,17,29]; telecom frequency conversion has also been employed to extend the distance of remote entanglement [28].

When atomic ensembles are employed as quantum memories, they are typically modeled as noninteracting atoms, and collision between atoms are unfavorable. In this situation, the preparation of entanglement with a single photon is probabilistic, and the preparation probability is kept very low, typically to minimize the contribution of high-order events [4,5]. However, Rydberg interaction provides a promising solution to create entanglement deterministically [30,31], as a single atom excited in a Rydberg state can block further excitations into the Rydberg state [32,33]. In recent years, plenty of research has been performed on Rydberg quantum optics [34–49]. In particular, Li *et al.* [38] demonstrated entanglement between a Rydberg excitation and a number-state encoded light field. The number-state encoding suffers from being phase sensitive. To avoid this, Li *et al.* realized entanglement between a Rydberg excitation and a polarization encoded single photon [48]. This scheme nevertheless succeeds merely 50% in principle, limiting its efficiency in entangling remote nodes [28,50] via entanglement swapping [51].

In this Letter, we propose and experimentally realize a scheme that entangles an atomic ensemble with a single photon's time-bin modes deterministically. The detailed scheme is depicted in Fig. 1. We consider a mesoscopic atomic ensemble in the regime of full blockade [33]. All atoms initially stay in a ground state $|g\rangle$. Two Rydberg levels $|r_1\rangle$ and $|r_2\rangle$ are employed to host a collective excitation. Our scheme starts from a Rydberg state preparation phase, in which we first apply a collective $\pi/2$ pulse coupling $|g\rangle$ and $|r_1\rangle$ resulting in a collective state of $(|R_1\rangle + |G\rangle)/\sqrt{2}$, and apply a subsequent π pulse coupling $|g\rangle$ and $|r_2\rangle$ resulting in a superposition state of $(|R_1\rangle + |R_2\rangle)/\sqrt{2}$, where $|G\rangle$ denotes all atoms in $|g\rangle$ and $|R_j\rangle = N^{-1/2}\sum_{i=1}^{N}|g^1 g^2 \cdots r_j^i \cdots g^N\rangle$ denotes a collective excitation in $|r_j\rangle$, with N being number of atoms and i being an atom index. We name the second π pulse as a "patching" pulse, since it creates a full excitation out of a half excitation, harnessing the Rydberg blockade between $|r_1\rangle$ and $|r_2\rangle$. In the next phase of our scheme, atom-photon

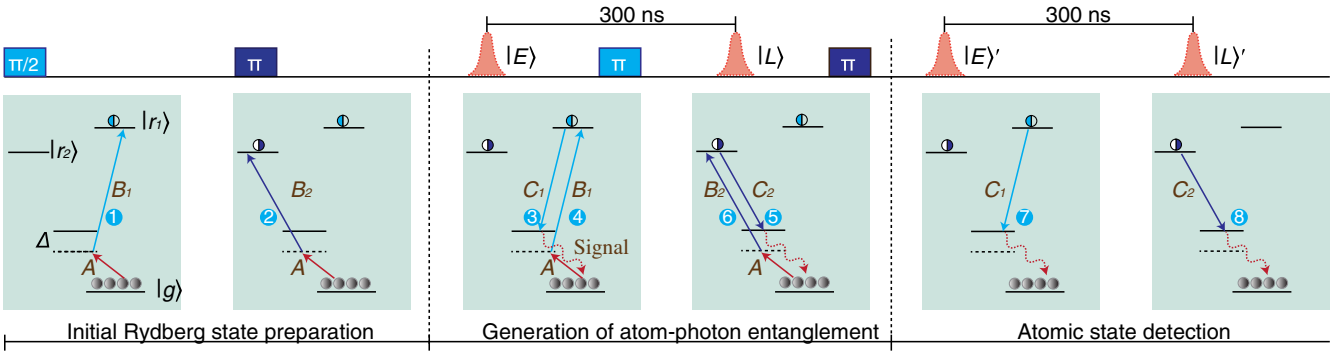

FIG. 1. Scheme of generating deterministic time-bin entanglement. In the first phase, we prepare a Rydberg superposition state $(|R_1\rangle + |R_2\rangle)/\sqrt{2}$. In the second phase, we apply the cyclical "retrieving and patching" process for $|R_1\rangle$ and $|R_2\rangle$ in sequence, which results in a retrieval photon whose temporal mode is entangled with the Rydberg levels of the collective excitation. In the last phase, we detect the atomic state via retrieving it to the temporal mode of a second photon. The excitation and patching process involve a two-photon Raman process. Spatial arrangement of the Raman beams is shown in Fig. 2. Numerically filled circles indicate relative time sequences of all the steps.

entanglement is generated via a cyclical process of "retrieving and patching." We first retrieve $|R_1\rangle$ to a single photon and patching it back by applying a π pulse coupling $|g\rangle$ and $|r_1\rangle$. The Rydberg blockade between $|r_1\rangle$ and $|r_2\rangle$ again plays a key role, ensuring that a $|R_1\rangle$ excitation is recreated only if there was a $|R_1\rangle$ excitation previously. Afterwards, we apply the retrieving and patching process for $|R_2\rangle$, creating a photon in a delayed temporal mode. After these steps, the joint atom-photon state can be expressed as

$$|\Psi\rangle_{ap} = (1/\sqrt{2})(|R_1\rangle|E\rangle + |R_2\rangle|L\rangle), \tag{1}$$

where $|E\rangle$ or $|L\rangle$ denotes a single photon in the temporal early or late mode. We note that all the atomic manipulation steps are deterministic. The retrieving process from a Rydberg excitation to a single photon [52] is also deterministic in principle, as long as the optical depth is high enough. Thus we claim that our scheme is deterministic, which differentiates from the traditional Duan-Lukin-Cirac-Zoller scheme [5] that creates entanglement probabilistically through spontaneous Raman scattering. In the last phase, we retrieve the atomic state $|R_1\rangle$ and $|R_2\rangle$ in sequence to a second photon in the temporal mode of $|E\rangle'$ and $|L\rangle'$ to verify the entanglement.

Our experimental setup is illustrated in Fig. 2. An ensemble of ^{87}Rb atoms is captured by a conventional magneto-optical trap (MOT) lasting 30 ms, and a following dark spontaneous force optical trap (dark SPOT) [53,54] lasting 70 ms. Afterwards, the atoms are loaded into an optical dipole trap formed by a 1064 nm laser propagating along the y direction with a power of 2 W and a waist of 5 μm in the x direction and 25 μm in the z direction, resulting in an optical depth of 1.7 along the x direction and a density of 10^{11} cm^{-3}. The energy levels include a ground state $|g\rangle = |5S_{1/2}, F = 2, m_F = +2\rangle$, an intermediate state $|e\rangle = |5P_{1/2}, F = 1, m_F = +1\rangle$, and two Rydberg states $|r_1\rangle = |81S_{1/2}, m_j = +1/2\rangle$ and $|r_2\rangle = |81S_{1/2}, m_j = -1/2\rangle$. We employ a two-photon Raman process to excite an atom to a Rydberg level, involving a 795 nm laser and a 474 nm laser. Single-photon detuning is set to $\Delta/(2\pi) = -40$ MHz. The two Rydberg levels are selected to be close to each other. Thus we are able to share the same 474 nm laser instead of seeking a second blue laser for the other Rydberg state. Typical collective Rabi oscillations measured for the two Rydberg states are plotted in Fig. 2(a), with more details given in the Supplemental Material [55]. Determined by the phase-matching condition [52], retrieved single photons propagate in the x direction, which is the same as the 795 nm Raman laser. At the same time, the single photons also have the same polarization as the Raman laser, thus slight leakage of the Raman laser will spoil the single photons. In our experiment, we solve this problem by using a temporal filter involving an acousto-optic modulator (AOM$_1$) in Fig. 2(b) to deflect the optical field only when retrieving the single photons. Afterwards, the single photon enters an active unbalanced Mach-Zehnder (MZ) interferometer, in which the $|E\rangle$ mode goes through the long arm while the $|L\rangle$ mode goes through the short arm. The MZ interferometer is employed not only to measure the first photon but also the second photon retrieved for atomic state detection, which is enabled with an optical switch [AOM$_2$ in Fig. 2(b)]. Finally, the photons are measured with single-photon detectors (SPDs) and analyzed in polarization.

Before characterizing the atom-photon entanglement, it is crucial to verify that the "patching" process is coherent and a Rydberg excitation is genuinely created in a superposition state. Therefore, we first perform an experiment that retrieves the atomic excitation immediately after its creation. In other words, we skip the second phase in Fig. 1. Thus the initial atomic state $(|R_1\rangle + |R_2\rangle)/\sqrt{2}$ is directly converted to $(|E\rangle' + e^{i\phi}|L\rangle')/\sqrt{2}$, with an internal phase ϕ

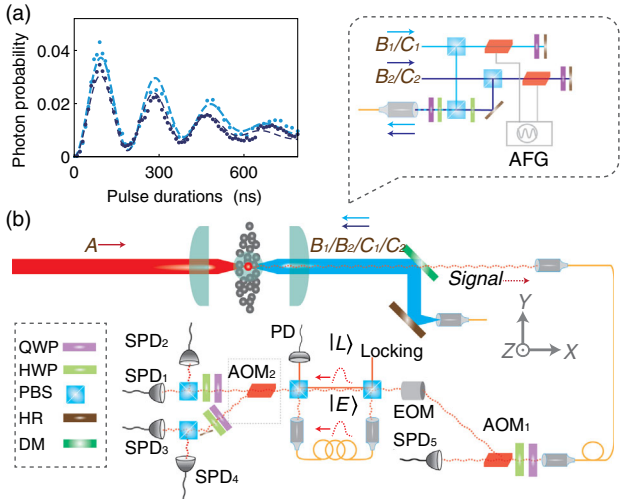

FIG. 2. Experimental setup. (a) Observed collective Rabi oscillations. Light blue dots represent the oscillation between $|G\rangle$ and $|R_1\rangle$ and dark blue dots represent the oscillation between $|G\rangle$ and $|R_2\rangle$. Dashed lines are the fitting results, indicating a π pulse duration of 92.95 ns and 92.18 ns for $|R_1\rangle$ and $|R_2\rangle$, respectively. (b) Layout of the experiment. The 795 nm beam counterpropagates with the 474 nm beams, all of which are tightly focused to address a small region of the atomic cloud to define a mesoscopic ensemble with full blockade (more details available in [56]). Single photons are retrieved in the x direction, and are afterwards subjected to fiber coupling, temporal filtering, interfering through an unbalanced MZ interferometer, switching, rotating in polarization, and final detecting sequentially. The fibers used in the two arms of the MZ interferometer are 65 m and 5 m which give a relative photon delay of about 300 ns. The interferometer is actively stabilized by injecting a locking beam into the idle port. Our experiment involves four blue beams ($B_1/B_2/C_1/C_2$), which differentiate from each other in polarization, frequency, or both. We make use of a multiplexing scheme shown as the inset of Fig. 2(b) to adjust the frequencies dynamically and combine the beams into a single-mode fiber. AOM_2 is merely used for the Bell measurement. Polarization of the retrieved single photons is σ^-, which is later rotated to vertical (V) with the wave plates before AOM_1. The electro-optic modulator (EOM) preserves the vertical polarization for the $|E\rangle$ mode, while switches it to horizontal (H) for the $|L\rangle$ mode. Thus the interferometer makes an effective degree-of-freedom transformation of $|E\rangle \to |V\rangle$ and $|L\rangle \to |H\rangle$. The setting for the wave plates in front of the detectors varies for different measurement bases. Some abbreviations: half-wave plate (HWP), quarter-wave plate (QWP), polarizing beam splitter (PBS), high reflection mirror (HR), dichroic mirror (DM), photodiode (PD).

being dependent on the relative phases of B_1, B_2, C_1, and C_2. In order to get a stable phase, we make use of an arbitrary function generator (AFG) with dual outputs to control the AOMs for B_1/C_1 and B_2/C_2, respectively, as shown in the inset of Fig. 2(b), which sets a common phase for all four pulses. We perform measurement in the basis of $|\pm\rangle = (|E\rangle \pm |L\rangle)/\sqrt{2}$, with the result shown in Fig. 4(a). We vary the phase of C_1 and measure the single photon counts. As expected, the relative counts show as complementary sinusoidal oscillations as a function of phase. By fitting the result, we get an interference visibility of $V_{+/-} = 0.909 \pm 0.006$, which is mainly limited by inhomogeneity of the two temporal modes, optical misalignment, and detector afterpulse. The overall measured photon efficiency is about 1.7%, which includes preparation efficiency of a Rydberg excitation (~90%), retrieval efficiency (~13%), transmission and fiber coupling efficiency (~69%), AOM deflecting efficiency (~77%), transmission efficiency through the unbalanced MZ interferometer (~47%), and detector efficiency (~60%). We note that by harnessing enhancement with a low-finesse ring cavity [13], the retrieval efficiency may be improved significantly.

Next, we implement the whole scheme shown in Fig. 1. We add back the phase of atom-photon entanglement generation, by applying the retrieving and patching process for $|R_1\rangle$ and $|R_2\rangle$ in sequence, which creates a first photon that is entangled with atomic excitation in the form of $|\Psi\rangle_{ap}$. To verify the entanglement, we retrieve the atomic excitation as a second photon that entangles with the first photon in the form of $|\Psi\rangle_{pp} = (1/\sqrt{2})(|E\rangle|E\rangle' + e^{i\psi}|L\rangle|L\rangle')$, with an internal phase ψ dependent on the Raman and retrieving fields. To verify the entanglement, we perform the correlation measurement both in the eigenbasis of $|E\rangle/|L\rangle$, and in a superposition basis of $|+\rangle/|-\rangle$. The detectors SPD_1 and SPD_2 are employed for this measurement through temporal multiplexing, and measurement settings are configured by rotating the wave plates. Measured temporal profiles for the four modes are shown in Fig. 3 together will the control pulses. We give coincidence measurement results in Fig. 4(b). As expected, when we vary the internal phase ψ linearly, coincidences in the eigenbasis show no dependence, while coincidences in the superposition basis show as sinusoidal oscillations.

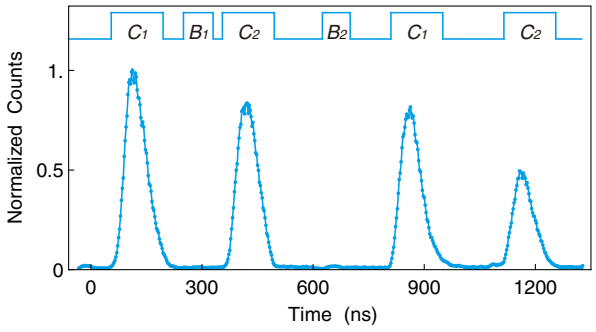

FIG. 3. Temporal profile for the single photons. Pulse labels in the time sequence are defined in Fig. 1. Measurement is performed in the eigenbasis of $|E\rangle/|L\rangle$. Temporal delays through the unbalanced interferometer are corrected to differentiate different time-bin modes. The four peaks in the profile refer to the modes of $|E\rangle$, $|L\rangle$, $|E\rangle'$, and $|L\rangle'$ in sequence. Amplitudes for the last two modes are slightly smaller, which is mainly due to incomplete retrieval of the Rydberg excitations.

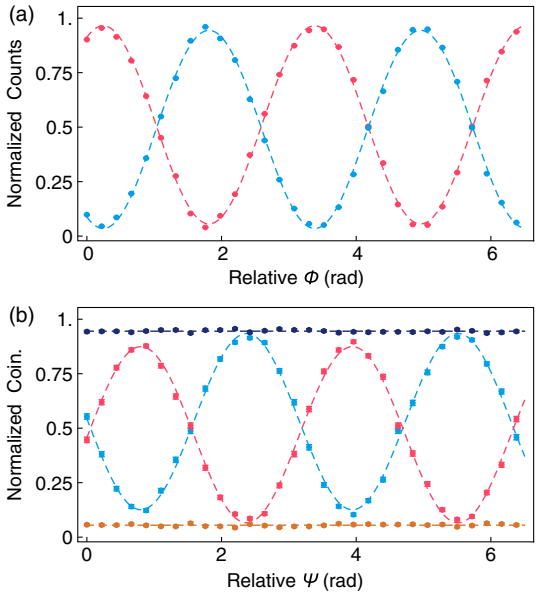

FIG. 4. Photon counting result. (a) Verification of the initial Rydberg state preparation. $(|R_1\rangle + |R_2\rangle)/\sqrt{2}$ is converted to $(|E\rangle' + e^{i\phi}|L\rangle')/\sqrt{2}$ and measured in the basis of $(|E\rangle' \pm |L\rangle')/\sqrt{2}$. Dependence on the internal phase ϕ is plotted. Dashed lines are the fitting results. (b) Characterization of the entanglement $|\Psi\rangle_{pp} = (1/\sqrt{2})(|E\rangle|E\rangle' + e^{i\psi}|L\rangle|L\rangle')$ via correlation measurement. In the eigenbasis, the sum of $|E\rangle|E\rangle'$ and $|L\rangle|L\rangle'$ coincidences is shown in dark blue, while the sum of $|E\rangle|L\rangle'$ and $|L\rangle|E\rangle'$ coincidences is shown in orange. In the superposition basis, the sum of $|+\rangle|+\rangle'$ and $|-\rangle|-\rangle'$ coincidences is shown in red, while the sum of $|+\rangle|-\rangle'$ and $|-\rangle|+\rangle'$ is shown in light blue. The dashed lines are the fitting results.

By fitting the results, we get a visibility of $V_1 = 0.890 \pm 0.010$ for the eigenbasis, and $V_2 = 0.811 \pm 0.008$ for the superposition basis, which together give an entanglement fidelity as $F \approx (1 + V_1 + 2V_2)/4 = 0.878 \pm 0.005$ [57]. A moderate visibility in the superposition basis contributes most for the entanglement infidelity. Feasible measures for improvement include using faster switches, using detectors with a lower probability of afterpulse, and using two Rydberg levels of different principal quantum number to reduce crosstalk.

Finally, we verify the entanglement directly via testing the Bell-CHSH inequality [58,59]. In this test, the two photons need to be measured in different settings, thus the previous detector multiplexing scheme does not work. We make use of an active switcher (AOM_2) to solve this problem. The AOM lets the first photon pass through and directs it to SPD_1 and SPD_2, while deflecting the second photon and directing it to SPD_3 and SPD_4. To perform the Bell test, we need to measure the S parameter that is defined as $S = |E(\alpha,\beta) + E(\alpha^*,\beta) + E(\alpha,\beta^*) - E(\alpha^*,\beta^*)|$, with $E(\alpha,\beta)$ being the joint expectation value when one photon is measured in the α setting and the other photon is measured in the β setting. A setting θ refers to a measurement in the basis of $|\theta\rangle = \cos(\theta)|E\rangle + \sin(\theta)|L\rangle$ and $|\theta^\perp\rangle = \sin(\theta)|E\rangle - \cos(\theta)|L\rangle$. $E(\alpha,\beta)$ takes a maximal value 1 for perfect parallel correlation, and -1 for perfect anticorrelation. For perfect entanglement and optimized settings, the S parameter can take a maximal value of $2\sqrt{2}$. The threshold to certify entanglement is $S > 2$. We set the internal phase ψ of $|\Psi\rangle_{pp}$ to 0 and perform the measurements. The results are shown in Table I, and we get $S = 2.173 \pm 0.055$, which violates the inequality by 3.16 standard deviations.

TABLE I. Measurement results for Bell-CHSH test.

α, β	22.5, 45	22.5, 0	67.5, 45	67.5, 0
$E(\alpha,\beta)$	−0.415	−0.531	−0.568	0.659
σ_E	0.029	0.028	0.026	0.025

In summary, we propose and experimentally realize a scheme of deterministic time-bin entanglement between a single photon and a mesoscopic atomic ensemble. We harness two Rydberg levels to host a collective atomic qubit, and employ a cyclical retrieving and patching process to create atom-photon entanglement. Self-blockade in each Rydberg level, and cross blockade between the two levels play key roles for the scheme. Our experiment fully implements the scheme. Via performing correlation measurements, we estimate an entanglement fidelity of 87.8%. We also perform a Bell inequality test to verify the entanglement directly. Further improvements include using a low-finesse cavity to improve the retrieval efficiency [7,13], transferring the atomic qubit from Rydberg levels to ground state levels [41,43], and using an optical lattice to achieve long-lived storage [17,29], etc. With these developments, the atom-photon entanglement created in our work may become a strong candidate as a fundamental element for constructing large-scale quantum networks [1–4].

This work was supported by National Key R&D Program of China (No. 2017YFA0303902), Anhui Initiative in Quantum Information Technologies, National Natural Science Foundation of China, and the Chinese Academy of Sciences.

*These authors contributed equally to this work.

[1] H. J. Kimble, Nature (London) **453**, 1023 (2008).
[2] C. Simon, Nat. Photonics **11**, 678 (2017).
[3] S. Wehner, D. Elkouss, and R. Hanson, Science **362**, eaam9288 (2018).
[4] N. Sangouard, C. Simon, H. de Riedmatten, and N. Gisin, Rev. Mod. Phys. **83**, 33 (2011).
[5] L.-M. Duan, M. Lukin, J. I. Cirac, and P. Zoller, Nature (London) **414**, 413 (2001).
[6] K. Hammerer, A. S. Sørensen, and E. S. Polzik, Rev. Mod. Phys. **82**, 1041 (2010).

[7] J. Simon, H. Tanji, J. K. Thompson, and V. Vuletić, Phys. Rev. Lett. **98**, 183601 (2007).

[8] B. Zhao, Y.-A. Chen, X.-H. Bao, T. Strassel, C.-S. Chuu, X.-M. Jin, J. Schmiedmayer, Z.-S. Yuan, S. Chen, and J.-W. Pan, Nat. Phys. **5**, 95 (2009).

[9] R. Zhao, Y. Dudin, S. Jenkins, C. Campbell, D. Matsukevich, T. Kennedy, and A. Kuzmich, Nat. Phys. **5**, 100 (2009).

[10] S.-Y. Lan, A. G. Radnaev, O. A. Collins, D. N. Matsukevich, T. A. Kennedy, and A. Kuzmich, Opt. Express **17**, 13639 (2009).

[11] Y. O. Dudin, A. G. Radnaev, R. Zhao, J. Z. Blumoff, T. A. B. Kennedy, and A. Kuzmich, Phys. Rev. Lett. **105**, 260502 (2010).

[12] A. G. Radnaev, Y. O. Dudin, R. Zhao, H. H. Jen, S. D. Jenkins, A. Kuzmich, and T. A. B. Kennedy, Nat. Phys. **6**, 894 (2010).

[13] X.-H. Bao, A. Reingruber, P. Dietrich, J. Rui, A. Dück, T. Strassel, L. Li, N.-L. Liu, B. Zhao, and J.-W. Pan, Nat. Phys. **8**, 517 (2012).

[14] Y. O. Dudin, L. Li, and A. Kuzmich, Phys. Rev. A **87**, 031801(R) (2013).

[15] Z. Xu, Y. Wu, L. Tian, L. Chen, Z. Zhang, Z. Yan, S. Li, H. Wang, C. Xie, and K. Peng, Phys. Rev. Lett. **111**, 240503 (2013).

[16] Y.-W. Cho, G. T. Campbell, J. L. Everett, J. Bernu, D. B. Higginbottom, M. T. Cao, J. Geng, N. P. Robins, P. K. Lam, and B. C. Buchler, Optica **3**, 100 (2016).

[17] S.-J. Yang, X.-J. Wang, X.-H. Bao, and J.-W. Pan, Nat. Photonics **10**, 381 (2016).

[18] Y.-F. Pu, N. Jiang, W. Chang, H.-X. Yang, C. Li, and L.-M. Duan, Nat. Commun. **8**, 15359 (2017).

[19] L. Tian, Z. Xu, L. Chen, W. Ge, H. Yuan, Y. Wen, S. Wang, S. Li, and H. Wang, Phys. Rev. Lett. **119**, 130505 (2017).

[20] R. Chrapkiewicz, M. Dabrowski, and W. Wasilewski, Phys. Rev. Lett. **118**, 063603 (2017).

[21] B.-S. Shi, D.-S. Ding, and W. Zhang, J. Phys. B **51**, 032004 (2018).

[22] Y.-F. Hsiao, P.-J. Tsai, H.-S. Chen, S.-X. Lin, C.-C. Hung, C.-H. Lee, Y.-H. Chen, Y.-F. Chen, I. A. Yu, and Y.-C. Chen, Phys. Rev. Lett. **120**, 183602 (2018).

[23] P. Vernaz-Gris, K. Huang, M. Cao, A. S. Sheremet, and J. Laurat, Nat. Commun. **9**, 363 (2018).

[24] Y. Wang, J. Li, S. Zhang, K. Su, Y. Zhou, K. Liao, S. Du, H. Yan, and S.-L. Zhu, Nat. Photonics **13**, 346 (2019).

[25] W. Chang, C. Li, Y.-K. Wu, N. Jiang, S. Zhang, Y.-F. Pu, X.-Y. Chang, and L.-M. Duan, Phys. Rev. X **9**, 041033 (2019).

[26] B. Jing, X.-J. Wang, Y. Yu, P.-F. Sun, Y. Jiang, S.-J. Yang, W.-H. Jiang, X.-Y. Luo, J. Zhang, X. Jiang, X.-H. Bao, and J.-W. Pan, Nat. Photonics **13**, 210 (2019).

[27] M. Cao, F. Hoffet, S. Qiu, A. S. Sheremet, and J. Laurat, Optica **7**, 1440 (2020).

[28] Y. Yu, F. Ma, X.-Y. Luo, B. Jing, P.-F. Sun, R.-Z. Fang, C.-W. Yang, H. Liu, M.-Y. Zheng, X.-P. Xie, W.-J. Zhang, L.-X. You, Z. Wang, T.-Y. Chen, Q. Zhang, X.-H. Bao, and J.-W. Pan, Nature (London) **578**, 240 (2020).

[29] X.-J. Wang, S.-J. Yang, P.-F. Sun, B. Jing, J. Li, M.-T. Zhou, X.-H. Bao, and J.-W. Pan, Phys. Rev. Lett. **126**, 090501 (2021).

[30] B. Zhao, M. Mller, K. Hammerer, P. Zoller, and M. Muller, Phys. Rev. A **81**, 052329 (2010).

[31] Y. Han, B. He, K. Heshami, C.-Z. Li, and C. Simon, Phys. Rev. A **81**, 052311 (2010).

[32] M. D. Lukin, M. Fleischhauer, R. Cote, L. M. Duan, D. Jaksch, J. I. Cirac, and P. Zoller, Phys. Rev. Lett. **87**, 037901 (2001).

[33] M. Saffman, T. G. Walker, and K. Molmer, Rev. Mod. Phys. **82**, 2313 (2010).

[34] T. Peyronel, O. Firstenberg, Q.-Y. Liang, S. Hofferberth, A. V. Gorshkov, T. Pohl, M. D. Lukin, and V. Vuleti, Nature (London) **488**, 57 (2012).

[35] Y. O. Dudin, L. Li, F. Bariani, and A. Kuzmich, Nat. Phys. **8**, 790 (2012).

[36] Y. O. Dudin and A. Kuzmich, Science **336**, 887 (2012).

[37] O. Firstenberg, T. Peyronel, Q.-Y. Liang, A. V. Gorshkov, M. D. Lukin, and V. Vuleti, Nature (London) **502**, 71 (2013).

[38] L. Li, Y. O. Dudin, and A. Kuzmich, Nature (London) **498**, 466 (2013).

[39] D. Tiarks, S. Baur, K. Schneider, S. Durr, and G. Rempe, Phys. Rev. Lett. **113**, 053602 (2014).

[40] H. Gorniaczyk, C. Tresp, J. Schmidt, H. Fedder, and S. Hofferberth, Phys. Rev. Lett. **113**, 053601 (2014).

[41] M. Ebert, A. Gill, M. Gibbons, X. Zhang, M. Saffman, and T. G. Walker, Phys. Rev. Lett. **112**, 043602 (2014).

[42] M. Ebert, M. Kwon, T. G. Walker, and M. Saffman, Phys. Rev. Lett. **115**, 093601 (2015).

[43] J. Li, M.-T. Zhou, B. Jing, X.-J. Wang, S.-J. Yang, X. Jiang, K. Molmer, X.-H. Bao, and J.-W. Pan, Phys. Rev. Lett. **117**, 180501 (2016).

[44] H. Gorniaczyk, C. Tresp, P. Bienias, A. Paris-Mandoki, W. Li, I. Mirgorodskiy, H. P. Bchler, I. Lesanovsky, and S. Hofferberth, Nat. Commun. **7**, 12480 (2016).

[45] J. D. Thompson, T. L. Nicholson, Q.-Y. Liang, S. H. Cantu, A. V. Venkatramani, S. Choi, I. A. Fedorov, D. Viscor, T. Pohl, M. D. Lukin, and V. Vuleti, Nature (London) **542**, 206 (2017).

[46] H. Busche, P. Huillery, S. W. Ball, T. Ilieva, M. P. A. Jones, and C. S. Adams, Nat. Phys. **13**, 655 (2017).

[47] D. Tiarks, S. Schmidt-Eberle, T. Stolz, G. Rempe, and S. Drr, Nat. Phys. **15**, 124 (2019).

[48] J. Li, M.-T. Zhou, C.-W. Yang, P.-F. Sun, J.-L. Liu, X.-H. Bao, and J.-W. Pan, Phys. Rev. Lett. **123**, 140504 (2019).

[49] S. H. Cantu, A. V. Venkatramani, W. Xu, L. Zhou, B. Jelenkovi, M. D. Lukin, and V. Vuleti, Nat. Phys. **16**, 921 (2020).

[50] Z.-S. Yuan, Y.-A. Chen, B. Zhao, S. Chen, J. Schmiedmayer, and J.-W. Pan, Nature (London) **454**, 1098 (2008).

[51] J.-W. Pan, D. Bouwmeester, H. Weinfurter, and A. Zeilinger, Phys. Rev. Lett. **80**, 3891 (1998).

[52] M. Saffman and T. G. Walker, Phys. Rev. A **66**, 065403 (2002).

[53] W. Ketterle, K. B. Davis, M. A. Joffe, A. Martin, and D. E. Pritchard, Phys. Rev. Lett. **70**, 2253 (1993).
[54] C. G. Townsend, N. H. Edwards, K. P. Zetie, C. J. Cooper, J. Rink, and C. J. Foot, Phys. Rev. A **53**, 1702 (1996).
[55] See Supplemental Material at http://link.aps.org/supplemental/10.1103/PhysRevLett.128.060502 for a discussion on atom number variance and collective Rabi oscillation.
[56] M.-T. Zhou, J.-L. Liu, P.-F. Sun, Z.-Y. An, J. Li, X.-H. Bao, and J.-W. Pan, Phys. Rev. A **102**, 013706 (2020).
[57] O. Ghne and G. Tth, Phys. Rep. **474**, 1 (2009).
[58] J. S. Bell, Rev. Mod. Phys. **38**, 447 (1966).
[59] J. F. Clauser, M. A. Horne, A. Shimony, and R. A. Holt, Phys. Rev. Lett. **23**, 880 (1969).